Looking into the green roof scenario to mitigate flash flood effects in Mamak, Turkey, via classifying images of Sentinel-1, 2, and PlanetScope satellites with LibSVM algorithm in Google Earth Engine cloud platform

SİMA POUYA[1], MAJİD AGHLMAND[2], FEVZİ KARSLİ[3]

---

[1] Inonu University, Faculty of Fine Arts and Design, Department of Landscape Architecture, Malatya, Turkey; e-mail: sima.pouya@inonu.edu.tr
[2] Eskisehir Technical University, Civil Engineering Department, Eskisehir, Turkey; e-mail: meecitt@gmail.com, maghlmand@eskisehir.edu.tr
[3] Karadeniz Technical University, Department of Geomatics, Trabzon, Turkey; e-mail: fkarsli @ktu.edu.tr

ABSTRACT   This research aimed to increase the green space factor to mitigate flash flood effects on urban storm water runoff in the Ankara Mamak region and to minimize the damages by flash floods. The land use/cover map was first obtained by using the images of Sentinel-1, Sentinel-2, and PlanetScope satellites with the LIBSVM algorithm on the Google Earth Engine. The GSF value was then calculated and it was low (0.26) compared to world standards. This study was proposed as a solution for the flood disaster, using the extensive green roof scenario. After green roof conversion scenarios, the GSF value was recalculated. It was found to be above the minimum of green infrastructure that human settlements should achieve, regardless of density or land use (0.43). Offering high resolution images and the possibility of processing them via different algorithms of machine learning has revolutionized the environmental and urban-related studies as they help urban managers and planners to make decisions accurately and quickly.

KEY WORDS   Google Earth Engine – Sentinel 1 – Sentinel 2 – PlanetScope – Green spaces factor – flash floods – green roofs – Ankara/Mamak district

1. Introduction

In recent years, one of the most visible disasters in the world has been flooding events. The flood disaster brings with it many negative consequences, the most important of which is damage to urban infrastructures and agricultural lands, and even causing loss of life (Swan 2010; Tavus et al. 2018). With the gradual decrease of vegetation in cities and the increase of impermeable surfaces, water basins are insufficient in terms of storage capacity. As a result, precipitation causes an increase in surface runoff, and the increase in this runoff in urbanization areas causes the deterioration of river embankments, erosion of slopes, flash floods to appear more frequently, and infrastructures to be exposed to flooding (Shuster et al. 2005). Urban development increases the asphalt roads and roofs and then changes the hydrology of urban areas. An impermeable surface cannot absorb rainwater. Water flows from closed surfaces and reduces underground drinking water. Excessive rainfall and rainwater exceeds the channel capacities and increases the likelihood of flooding, resulting in property damage (Barnes, Morgan, Roberge 2001; Brudermann, Sangkakool 2017; Lee et al. 2013).

2. Review of The Green Space Factor

The Green Space Factor (GSF), which was first developed in Germany, has been applied in many countries. A calculation formula has been created for this value. A factor has been assigned to different types of surface coatings. Factors include the ecosystem services of each surfacing; It is given in terms of contributing to the soil, vegetation, and water, and more according to the rainwater infiltration potential. The reason for this is that the water holding capacity of the surface cover is natural and healthy, adapting to climate change, improving air quality, protecting biological diversity, and providing ecosystem benefits. Factors between 0–1 were determined for other surfaces by assigning a factor of 0 to impermeable surfaces such as concrete and asphalt, and a factor of 1 to surfaces with deep soils and the most natural vegetation (Jansson 2014).

For any development planning in urban areas, the GSF value must first be calculated and then compared with the GSF value after development. Evaluation, mapping, and measurement of new types of surface coatings are of great importance (Table 1). Typical surface types by the countries that make GSF applications; described as waterproof surfaces, permeable pavement, meadow areas, trees and bushes, green roofs, green vertical gardens, etc. They are then assigned a value and a factor based on their contribution to the ecosystem service. To calculate the GSF value, the factor of each surface coverage in an area is multiplied by the total

Table 1 – Proposed surface cover type descriptions and factors

Surface Cover Type	Factor
Semi-natural vegetation (e.g. woodland, flower-rich grassland) created on site	1.0
Wetland or open water (semi-natural, not chlorinated) created on site	1.0
Intensive green roof or vegetation over structure, Vegetated sections only, and Substrate minimum settled depth of 150 mm	0.8
Standard trees planted in natural soils or with a minimum of 25 cubic meters soil volume per tree (preferably with load-bearing substrates and connected pits)	0.8
Extensive green roof with the substrate of minimum settled depth of 80 mm (or 60 mm beneath vegetation blanket)	0.7
Flower-rich perennial planting	0.7
Rain gardens and other vegetated sustainable drainage elements	0.7
Hedges (line of mature shrubs one or two shrubs wide)	0.6
Standard trees planted in individual pits with less than 25 cubic meters of soil volume	0.6
Green wall–modular system or climbers rooted in the soil	0.6
Groundcover planting	0.5
Amenity grassland (species-poor regularly mown lawn)	0.4
Extensive green roof of sedum mat without substrate or other systems	0.3
Water features (chlorinated) or unplanted detention basins	0.2
Permeable paving	0.1
Sealed surfaces (e.g. concrete, asphalt, waterproofing, stone)	0.0

Source: Grant 2017

area of that cover and the sum of these values is divided by the general area of the site and the obtained value is accepted as the GSF value (as set out in formula 1 below; Jansson 2014).

The original formula for the GSF is:

$$\text{GSF} = \frac{\sum_{i=1}^{n}(F*a)}{A} \tag{1}$$

Where *F* is Factor which was determined according to the characteristics of each area, a is Area of each Factor and *A* is Total Land Area.

The purpose of the formation of GSF was that none of the new areas built and planned should fall below this standard. Therefore, green roofs and green walls are used as alternatives to improve this value in dense urban areas(Julie, Kragh 2017). In most cases, the absolute minimum GSF target is 0,3, which is believed to correspond to a minimum of green infrastructure that human settlements should achieve, regardless of density or land use. However, a minimum target of 0.5–0.6 is often set for new developments, where there is still room for achieving higher environmental quality at the design stage (Vartholomaios et al. 2013).

3. Increasing the GSF and decreasing stormwater by extensive green roof scenarios

Stormwater management has traditionally been done by increasing the water supply capacity of underground facilities. However, in the last 25 years, stormwater management methods have started to be used to keep the water in place. Thus, it causes to reduce the flow volume. Recently, current strategies such as rain gardens, vegetative ditches, and green roofs have been involved in stormwater management. Thanks to these strategies, it provides advantages in water retention, storage, infiltration, and pre-treatment. These methods have also been less costly, easier to maintain and more ecologically beneficial structures than traditional infrastructure solutions (Barr et al. 2017).

Many studies have determined the reduction of rainwater flow of green roofs with different studies (Berndtsson 2010; Beyhan, Erbas 2013). It is known that one of the problems that might arise with rapid urbanization in cities like Ankara is the transformation of excessive precipitation into floods. Due to the rapidly increasing population and construction, the soil and green vegetation that absorbs the rain water in the cities is decreasing. However, the surfaces that immediately transfer the water coming on them to the drains and from there to the sewer or rain discharge system are increasing. The simultaneous discharge of all rainwater falling on the city can lead to flood disasters with the increase in the amount of precipitation. Green roofs are vital at this point. Green roofs can absorb rain water, reducing excessive water transmission to the soil, and delaying the transportation of rain water falling on the roof surface to the drainage system for up to an hour. This delay plays an important role in reducing the risk of flooding.Although green roof is not the final and complete solution, but due to its ability to be implemented in a shorter period of time and by citizens, it can play an appropriate and significant role along with macro policies to combat the effects of floods and runoff (Atik et al. 2013; Esringü, Toy 2021).

Green roofs have been an effective system for the drainage and collection of rainwater. Generally, the roof of the buildings in urban areas covers a large area of the city, so it has an important potential to create green areas (Van Woert et al. 2005). It is a system whose green roofs prevent rainwater from entering the building and meet its water needs with rainwater. Green roofs started to be used in Germany at first and then started to be applied in the United States to form roof surfaces onto permeable surfaces (Barr et al. 2017).

By the green roofs, it is possible to make the impermeable roof surfaces permeable. The green roof absorbs water and slowly leaves, some of it is kept in the atmosphere by evaporation by holding it by the vegetation. The remaining water moves away from the system with roof drainage (Beyhan, Erbas 2013).

Green roofs can prevent flash floods by reducing the volume of drainage and keeping drainage below the peak (Shafique, Kim, Kyung-Ho 2018). Various studies have been conducted on the reduction of runoff by a green roof (Bengtsson, Grahn, Olsson 2005; Carter, Rasmussen 2006; Köhler et al. 2002; Li, Yeung 2014; Villarreal, Bengtsson 2005). For example, Hareret reported that a large green roof has the potential to hold 45%–55% of annual flow (Sozer et al. 2018). In a study conducted in two regions in Italy, it was revealed that the 68% flow volume of the green roof decreased. Therefore, green roof drainage can be a useful approach, especially in urban planning, to prevent flash flooding. In addition, since 30% of the surfaces in many cities are roofs, green roofs can be recommended to form these impermeable surfaces into permeable surfaces (Shafique, Kim, Kyung-Ho 2018).

Vanwoert et al. (2005), it was revealed that green roofs have the ability to retain more than 80% of the precipitation falling on the roof. Connelly, Liu (2005) determined that the water holding capacity of a green roof system planted with sedum species, with a 75 mm habitat, is between 86–94% in the dry season and 13–18% in the rainy season. This situation is related to the amount of moisture in the growing medium (Fioretti et al. 2010). In urban areas, green roofs retain rainwater longer and reduce runoff volume. At first, the incoming rainwater is stored in the soil layer, then it descends to the vegetation layer and is stored there so that the amount of water remaining in the ferry has decreased and the amount of water flow generated is considerably reduced. In addition, evapotranspiration, which is absent on typical roofs, allows evapotranspiration on green roofs (Shafique, Kim, Kyung-Ho 2018).

At the same time, there are several layers on green roofs. These layers also have benefits in increasing the quality of rainwater, saving energy, reducing the heat island effect, adding social and aesthetic value, and reducing air pollution (Van Woert et al. 2005).

These two types of roof gardens differ according to their characteristics, soil depth, plant variety, irrigation and maintenance demand, construction cost, weight, and construction purposes. Extensive green roofs are usually made to a depth of 4 inches (Fassman-Beck et al. 2013). On these roofs, grasshoppers such as sedum and drought-resistant plant species are generally preferred (Barr et al. 2017).

More structural systems are being built on Intensive green roofs and soil depth is over 12 inches and it is important to prepare the environments for large trees to grow. The planning of this type of green roof should be done together with the building application, whereas supporting systems may be needed depending on the age and weight-bearing capacity of the main roof. In addition, it is important that these additions cause minimum damage to the building and have a negative impact (Barr et al. 2017).

Many countries around the world have adopted these benefits of roof gardens in urban development and roof garden applications are quite common (Jafari et al. 2015). The roof garden in Turkey; Although it has started to attract the attention of users and designers since it started to be evaluated in terms of climatic changes and energy efficiency, there is not enough work on the subject due to insufficient budget allocated to environmental problems due to economic Problems (Düzenli 2018).

Flood disaster in Turkey has been one of the most destructive natural disasters after landslides and earthquakes. One of the most visible areas of the flood disaster was the province of Ankara. In 2018, at least 5 flood events were seen in this city. The increase in flood events due to climate change in Turkey is expected in the next ten years. Therefore, it is extremely necessary to take the necessary precautions and make preparations before the flood disaster occurs again (Koç, Natho, Thieken 2021; Sozer et al. 2018).

4. Remote sensing and urban studies

Progress in technology and remote sensing science has made numerous changes in urban studies. Utilizing satellite images with high resolution has managed to resolve many of urban environment issues (Weng, Quattrochi 2006). Data amassed in this way can be applied in a wide range of research studies on mapping, monitoring, and modeling land. Important data can also be gathered by categorizing satellite images and producing Land Cover / Land Use (LCLU) maps.

Different studies have drawn on sentinel 1 and sentinel 2 satellite images. These two satellites have bands with resolutions of 10, 20, and 60 meters (Ienco et al. 2019). Sentinel 1 satellite data can increase the classification correction. PlanetScope satellite also presents images with resolution of 3 meters (Planet Team 2018). The images of this satellite has four bands, which are obtained daily (Sadeh et al. 2021). These images are typcally used to produce maps of land use. Additionally, these images can be used to extract varying indexes such as the normalized difference vegetation index (NDVI), The Pigment Specific Simple Ratio (PSSR), the Green Normalised Difference Vegetation Index (GNDVI), and Normalized difference water index (NDWI). These indexes increase the classification correction (Becker et al. 2021).

Different algorithims and methods might be used to produce land use and land map plans. SVM algorithm is one of them. The SVM algorithm is known as one of the successful algorithms (Poursanidis, Chrysoulakis, Mitraka 2015), and in the last 10 years many studies have used the SVM algorithm in nonparametric controlled classification studies (Foody, Mathur 2004; Li et al. 2020; Pal, Mather 2005). In the case of limited data, the SVM method gives much better results than other traditional methods such as Maximum Likelihood (Mantero, Moser, Serpico

2005; Mountrakis, Im, Ogole 2011). SVM performs the classification process using hyperplanes that best separate classes (Park et al. 2018). Google Earth Engine (GEE) is another progress that has recently been occurred in remote sensing.

GEE is a cloud platform that has brought about a revolution in access to remote sensing data and their analysis (Gorelick et al. 2017; Wang et al. 2020). The pre-processing stage of satellite images is done via GEE and the images become available for users in entirely free and prepared form. In GEE there is no need to download images. GEE also has the best algorithms of image process and can do the calculations in the parallel and simultaneous way on international scale (Becker et al. 2021, Praticò et al. 2021, Qu et al. 2021, Wang et al. 2020).

Studies have stated that green roof systems have the potential to keep the precipitation on the roof between 40–80% (Fioretti et al. 2010). During heavy rainfall, green roofs store water in their layers and transfer the remaining water to the drainage network after these layers are saturated. In this study, "How much does the creation of green roof surfaces affect the GSF quantity and what would be the fastest and most reliable method to make this calculation?" The answer to the question has been sought. The aim of this research is to increase the water-permeable surfaces and decrease the rainwater in Ankara/Mamak region, thus minimizing the damages caused by flash floods. In order to that, land use classification map was generated using remote sensing satellite images on the Google Earth Engine platform using the LIBSVM (A Library for Support Vector Machines) algorithm. The best way to form the roofs of buildings into permeable floats has been green roofs. The GSF value was then recalculated in the green roof scenario. The GSF value was encountered before and after the scenario and evaluated according to world standards.

5. Material and method

5.1. Research area

The city of Ankara is located at an altitude of 850 meters above the Ankara stream and Ankara plain. The Ankara plain is defined by a parallel mountain ridge running from west to east and closed on its northern, southern, and eastern edges. There are many streams and water rivers in the valleys. Ankara plain is surrounded by Hatip Stream from the east and İncesu Stream and other streams from the southeast (Kaymaz 2019). According to the Thornthwaite classification, the city of Ankara has a semi-arid mesothermal climate that faces water shortages in summer. According to Ankara Water and Sewage Administration (ASKİ), the water rate in Ankara dams is only 34,65% since 2019. For this reason, streams, valleys, and drainage infrastructures are of great importance in the sustainable urban

Table 2 – Average Number of Rainy Days and Average Monthly Total Rainfall (1991–2021)

Ankara	Jan	Feb	Mar	Apr	May	Jun	Jul	Aug	Sep	Oct	Nov	Dec
Average Number of Rainy Days	13.60	12.67	13.87	13.40	14.53	11.47	4.60	5.10	5.50	9.23	8.93	14.00
Average Monthly Total Rainfall (mm)	38.6	36.6	46.9	44.5	51.0	40.2	14.8	14.6	17.9	33.4	31.9	43.2

Source: Turkish State Meteorological Service (2022)

planning considered for Ankara. Their rivers have also damaged their environment mostly due to floods. The flood disaster along the Hatip Stream damaged the vegetable gardens in the surrounding Bentderesi, Dışkapı, Kazıkiçi regions and affected many places such as Akkopru, and loss of life was experienced. In addition, some of these streams have been heavily polluted, thus changing the urban landscape (Kaymaz 2019). In the flood event that occurred in Ankara on May 5th, 2018, many infrastructure houses and workplaces were damaged and caused many injuries (Figure 1c, 1d). Immediately after this disaster, two more flood events occurred in this city (May 20 and June 21, 2018; Tavus et al. 2018). The amount of rainfall in Ankara from 1991 to 2021 was higher in the first 6 months of the year (Table 2). The highest average rainfall is in May (51 mm).

Mamak District is positioned in the east part of Ankara, Turkey and subjected to rapid urban transformation (Fig. 1). Mamak area is the one part of the urban sprawl of Ankara like Etimesgut, Gölbaşı, Pursaklar, Sincan etc. Almost 640 thousand people live in this region. Mamak has an important part of the essential technical infrastructure in the city. Close proximity to the railway, highway, and other transportation options makes this part of the city a development focus. In addition to the transportation infrastructure, the east part of Mamak is used for recreational purpose in Bayındır Dam. There was some flooding in some parts of the Mamak District and it is known that other parts of the district are also prone to flooding. As mentioned by the Ankara Chamber of Civil Engineers, the Hatip Stream region, which is flooded is the region where the flood caused the most casualties of history (Yanar, Kocaman, Gokceoglu 2020).

The study area was selected by considering these conditions (Fig. 1). The region covers 321 km². The min elevation is 847 m and the max elevation is 1,913 m. Figure 1 (down) shows the basins, dem, and primary and secondary water paths. The modelling was done by NASA SRTM Digital Elevation 30 m (Farr et al. 2007) and ArcGis software. As the figure indicates, Bayindir Dam is also located in this eastern area of the research site. Mamak district is the district of Ankara that is most exposed to flood events. It seems that there are unplanned settlements in this region. For these reasons, the heavily urbanized area of the Mamak district was chosen as the research area.
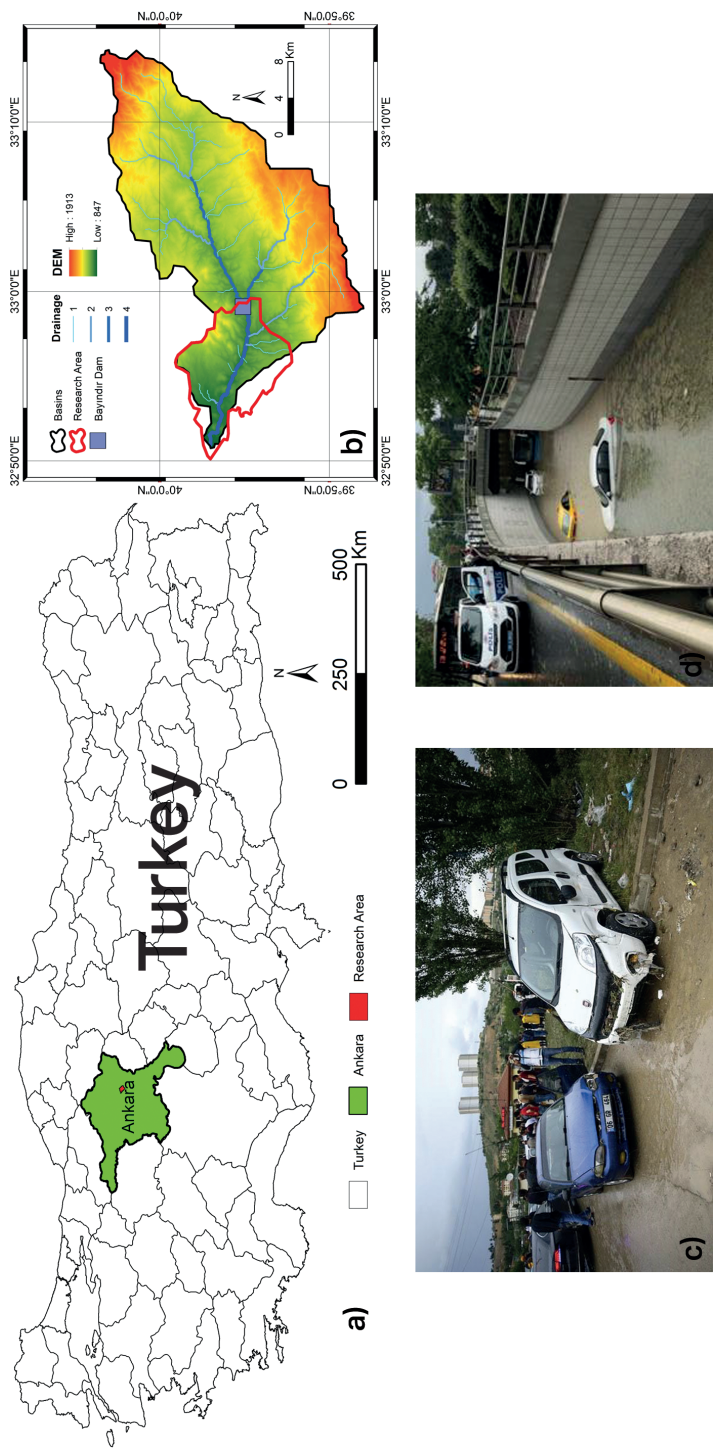
Fig. 1 – Research area location (up), examples of damages after the May 5th flood in Ankara (down, Tavus et al. 2018)

5.2. Methodology

The aim of this research is to increase the water-permeable surfaces and decrease the rainwater in Ankara/Mamak region, thus minimizing the damages caused by flash floods. In order to that, land use classification map was generated using remote sensing satellite images on the Google Earth Engine platform using The LIBSVM algorithm. The best way to form the roofs of buildings into permeable floats has been green roofs. The GSF value was then recalculated in the green roof scenario. The GSF value was encountered before and after the scenario and evaluated according to world standards.

In order to achieve the intended purposes, the under study zone was classified to reach the area of each of the following classes.

(1) Woodland / trees on deeper soil,
(2) Tree in shallow soil / tree pit,
(3) Non Permeable Surface (road),
(4) Wetland or open water (semi-natural; not chlorinated) created on site,
(5) Non Permeable Surface (building) and
(6) Permeable Paving (soil or sand)

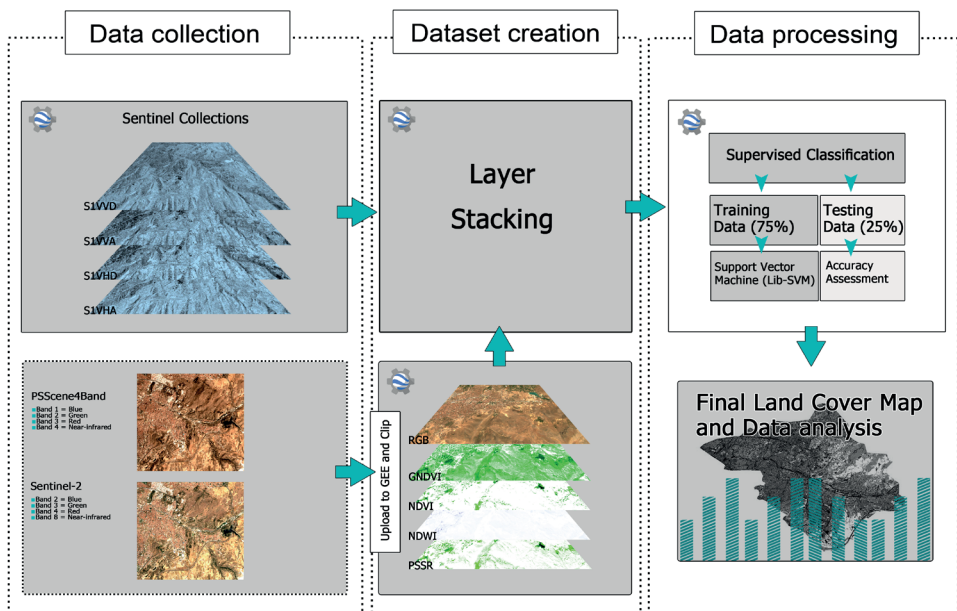Further, the study was designed in three steps: data collection, dataset creation, and data processing (Fig. 2).

Fig. 2 – Research flow diagram

5.3. Data Collection

In this research, the images of Sentinel-1, Sentinel-2, and PSScene4Band satellites have been used. Sentinel-1 and Sentinel-2 satellite images are available on the GEE platform. Additionally, the image related to PSScene-4Band was freely downloaded as aTiff file from the company website and was then uploaded to GEE.

5.3.1. Sentinel-1

The Sentinel-1 data is available on GEE (2021). Each scene was pre-processed with Sentinel-1 Toolbox using the following steps: (a) Thermal noise removal, (b) Radiometric calibration, (c) Terrain correction. In the present study, two images related to the dates 21.08.2020 and 22.08.2020 have been used. Both images have VV (Single co-polarization, vertical transmit / vertical receive) and VH (Dual-band cross-polarization, vertical transmit / horizontal receive) bands (S1B_ IW_GRDH_1SDV_20200821T035749_ 20200821T035814 _023016_02BB27_9FFC & S1B_IW_ GRDH_1SDV_20200822T 154226_20200822T154251 _023038_ 02BBE4_8FFF). The orbit direction is ascending in one of the imgaes and descending in another one (Fig. 3).
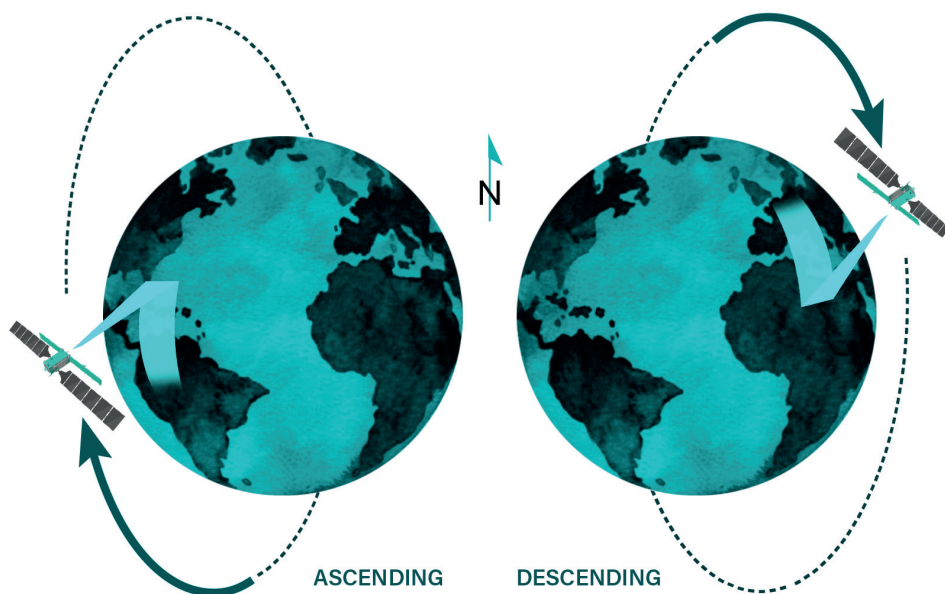

Fig. 3 – Sentinel-1; Ascending and Descending orbit

5.3.2. PlanetScope

The PlanetScope operated by Planet Labs, Inc (Planet Team 2018). The PlanetScope satellites have four spectral bands; Blue (455–515 nm), Green (500–590 nm), Red (590–670 nm), and NIR (780–860 nm; Sadeh et al. 2021). Planet Score satellite has taken images with 3 meters resolution (Planet Team 2018). In this research, the image "20200819 _081808_1010 _3B_AnalyticMS_SR" has been used.

5.3.3. Sentinel-2

Bands 2, 3, 4, and 8 of the Sentinel 2 satellite have a resolution of 10 meters, and these bands, along with other images, help to improve the classification accuracy (Ienco et al. 2019; *Sentinel-1*, n.d.) For the same purpose, in the present study, 10-meter image bands with the idea of "COPERNICUS/S2_SR/20200819T0836 11_20200819T084315_T36TVK" were used. This image is available as a Surface Reflection in GEE Database(GEE 2021).

5.4. Dataset Creation

Dataset was prepared in the GEE. The PSSceneBand satellite image, which has four bands, was placed in the dataset. With aims of increasing the accuracy of the classification. The normalized difference vegetation index (NDVI), The Pigment Specific Simple Ratio (PSSR), the Green Normalised Difference Vegetation Index (GNDVI), and Normalized difference water index (NDWI) was calculated and placed in the database (Table 3). Also, Sentinel-2 satellite with four bands and resolution of 10 meters (bands 2, 3, 4 and 8) were added to the dataset. Two images were also received from the Sentinel-1 satellite.

5.5. Data Processing

In this study, the LIBSVM algorithm (Chang 2011) was used. In this method, training points belonging to different classes are selected first. In this study, different classification areas were determined. These were: Vegetation-1(Woodland / trees on deeper soil), Vegetation-2 (Tree in shallow soil / tree pit), Road, Water, Build-up, and Bareland. The number of sample areas was determined via Formula 1 (Hu et al. 2016) given below. This formula is applied by determining points for each class.

In order to select the points and record their characteristics, the background image of GEE along with the image of PSScene4Band was used. 75% of the points were randomly selected for training and 25% for testing (Table 4).

Table 3 – Index information and formulas used in the study

Indexes	Formula	Indexes	Formula
NDVI (Jensen, Lulla 1987)	$\dfrac{NIR - Red}{NIR + Red}$	PSSR (Frampton et al. 2013)	$\dfrac{NIR}{Red}$
NDWI (Jensen, Lulla 1987)	$\dfrac{Green - Red}{Green + Red}$	GNDVI (Frampton et al. 2013)	$\dfrac{NIR - Green}{NIR + Green}$

Source: Jensen, Lulla (1987)

Table 4 – Classification information and numbers of points

No.	Class name	Training Points	Test Points	Color
1	Vegetation-1	675	225	
2	Vegetation-2	675	225	
3	Road	750	250	
4	Water	300	100	
5	Build-up	750	250	
6	Bareland	750	250	

$$N = \frac{Z^2(p)(q)}{E^2} \tag{2}$$

where p is the expected percent accuracy of the entire map, $q = 100 - p$, E is the allowable error, and $Z = 2$ from the standard normal deviate.

GEE makes it possible to do the calculations simultaneously and in parallel. The same possibility was used in the present study. In other words, simultaneous with dataset classification and LULC map production, the accuracy degree of the done classification was also assessed through Overall accuracy and Kappa coefficient.

In doing the classification, different scenarios were used and the highest accuracy was found to belong to Sentinel-2 (with four bands), Sentinel-1 (with four bands), PSS4 (with four bands), and indexes of NDVI + NDWI + GNDVI + PSSR (the Overall accuracy and Kappa were 98.26 and 97.79; Table 5).

Figure 4 shows the classification results. The two parts of a and b display the results of the two ranges more vividly.

5.6. The GSF calculation

All of the Surface Cover Type areas were gained in the GEE (Table 6). Then the GSF value was calculated according to the obtained classification map. To calculate a GSF for the site, the factor for a particular surface cover is multiplied by its

area (according to Table 1 proposed surface cover type factors were take). This is repeated for each surface cover type. The multiplied sums are added together and then divided by the overall site area (85,113,763 m²) to give an overall GSF score for a site of between 0 and 1. According to the 1 formula, the GSF value for case study are in this paper was 0.26.
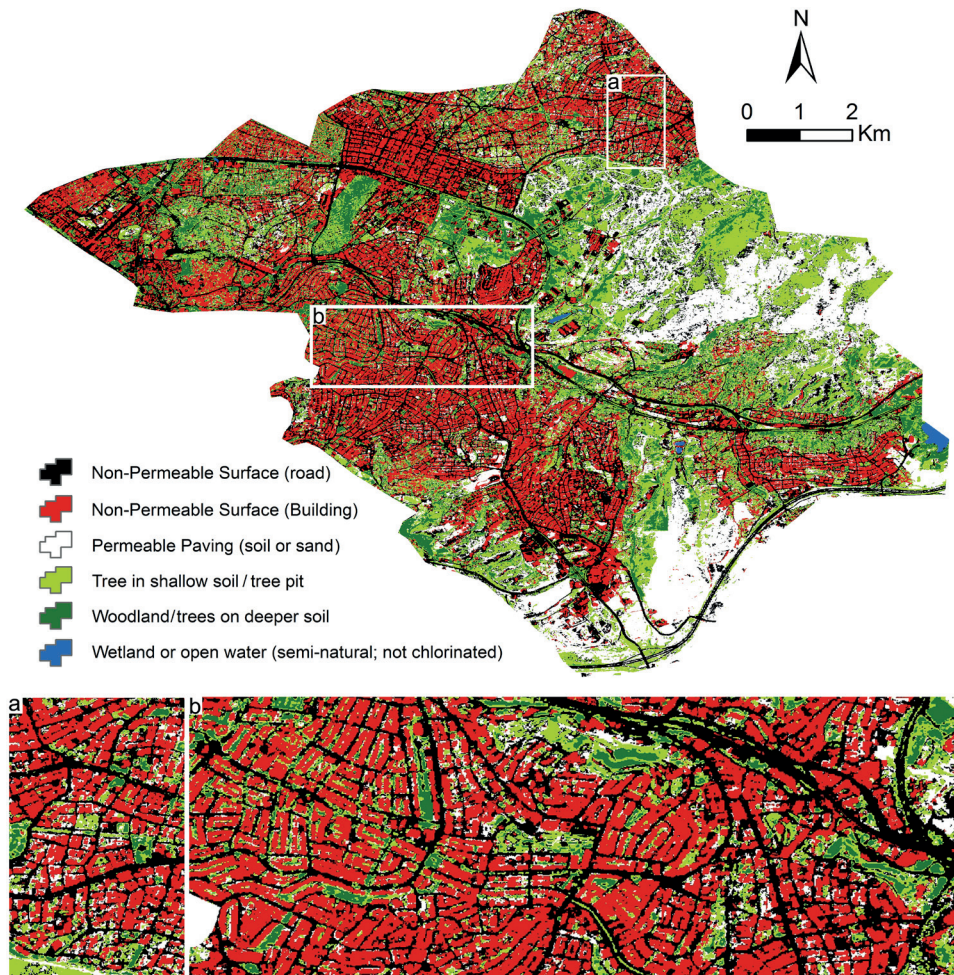

Fig. 4 – Classification results

Table 5 – Information pertinent to the dataset

No.	Combination	Band	Overall accuracy	Kappa coefficient
1	PSS4	4		
2	NDVI + NDWI + GNDVI + PSSR	4		
3	Sentinel-2	4	98.26	97.79
4	S1VVD + S1VHD	2		
5	S1VVA + S1VHA	2		

Table 6 – Surface cover type descriptions and factors in the case study of Mamak district

No.	Surface cover type	Factor	Area (m²)
1	Woodland / trees on deeper soil	1.0	6,569,397
2	Tree in shallow soil / tree pit	0.7	17,445,797
3	Non Permeable Surface (road)	0.0	23,088,847
4	Wetland or open water (semi-natural; not chlorinated) created on site	1.0	153,232
5	Non Permeable Surface (building)	0.0	20,547,687
6	Permeable Paving (soil or sand)	0.2	17,308,803
Total area			85,113,763

Table 7 – Calculated GSF before and after green roof conversion scenarios according to the result of classification by GEE

Class		Before Green Roof conversion scenarios			After Green Roof conversion scenarios		
		Area (m²)	Factor	Factor A × area	Area (m²)	Factor	Factor A × area
	Woodland/trees on deeper soil	6,569,397	1.0	6,569,397	6,569,397	1.0	6,569,397
	Tree in shallow soil/tree pit	17,445,797	0.7	12,212,057.9	17,445,797	0.7	12,212,057.9
	Non-Permeable Surface (road)	23,088,847	0.0	0.0	23,088,847	0.0	0.0
	Wetland or open water (semi-natural; not chlorinated)	153,232	1.0	153,232	153,232	1.0	153,232
	Non-Permeable Surface (Building)	20,547,687	0.0	0.0	0.0	0.0	0.0
	Permeable Paving (soil or sand)	17,308,803	0.2	3,461,760.6	17,308,803	0.2	3,461,760.6
	Extensive Green Roof	0.0	0.7	0.0	20,547,687	0.7	14,383,380.9
	GSF		0.26			0.43	

5.7. Green Roof conversion scenarios

According to the data obtained from the LCLU map in the study, it was determined that 51.27% of the research area has impermeable surfaces, and 47.08% of this rate belongs to the roofs of the buildings. There is no green roof example in the area for now, but the aim of this study was to put impermeable roof surfaces to permeable surfaces, namely the green roof scenario. After the green roof scenario, the GSF value was recalculated and this value increased from 0.26 to 0.43. The reason for this is that the factor given to green roofs has a high value and thus the GSF value has increased accordingly (Table 7, Fig. 5).

6. Discussion and conclusion

The use of remote sensing satellite imagery is very useful in regional research. PSScene4Band, Sentinel-2, and sentinel-1 images were used in this study. The images of the PSScene4Band satellite have a resolution of 3 meters and also the
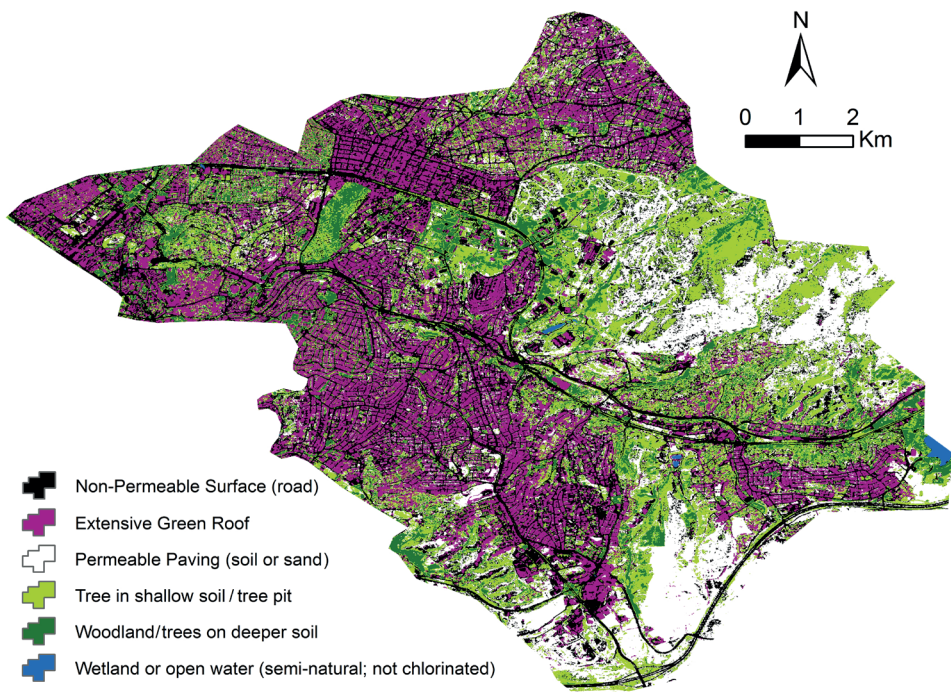

Fig. 5 – Classification result after Green Roof conversion scenarios in the Mamak district

imaging of this satellite is done daily, thus covering the gap that exists in other images of the satellite. The study also used GEE, which has a cloud platform. GEE has all the satellite images and its use of the cloud system helps to do all the analysis in the shortest time. The advent of the GEE cloud-computing platform makes it possible to access, manipulate, and analyze large volumes of geospatial datasets on the fly. The GEE cloud-computing platform also has a coding section and each user can code according to their purpose and desire. The possibility of coding in GEE has eliminated the need for GIS software and the whole process of research on this platform can be done for free.

The GSF value was calculated based on the obtained classification map. Obtained the GSF value is low (0.26) compared to world standards (In most cases the absolute minimum GSF target is 0.3). The analysis of LCLU map revealed that 51.27% of the case study area is covered with impervious surfaces (buildings and roads) and that roofs account for 24.14% of the total LCLU, and 47.08% of the impervious areas. Although no green roof installations are now present in the area, this study modeled – using extensive green roof details (conversion of 24.14% non-permeable to green roofs). After the green roof conversion scenarios, the GSF value was recalculated. According to Table 1, the factor of extensive green roofs is 0.7, so the new GSF value has increased to 0.42 which is above the minimum of green infrastructure that human settlements should achieve, regardless of density or land cover.

It causes flash flood events due to climate change in the world and especially in Turkey. The reasons for the mistakes made in urban planning were generally rapid urbanization, lack of appropriate infrastructure, and ignoring environmental factors. Flash floods in many parts of Ankara are considered as one of the most important natural disasters. Flood events damage infrastructure systems and natural assets. It is, then, necessary to take some measures to prevent this disaster in Ankara.

At this point, green roofs have important duties. It comes to mind as a solution address as a result of events that cause climate change such as heavy rain and flood events, high city temperatures, and atmospheric pollution. The point, however, to mention is that although green roofs alone are not enough to solve these problems (Dunnett, Kingsbury 2008), it offers measurable benefits. They are most useful in reducing or even eliminating water flow problems. Many studies have determined the reduction of rainwater flow of green roofs with different studies (Berndtsson 2010; Beyhan, Erbas 2013). Green roofs have been an effective system for the drainage and collection of rainwater. Generally, the roof of the buildings in urban areas covers a large area of the city, so it has an important potential to create green areas (Van Woert et al. 2005). By the green roofs, it is possible to make the impermeable roof surfaces permeable. The green roof absorbs water and slowly leaves, some of it is kept in the atmosphere by evaporation by holding it by the vegetation. Remaining water moves away from the system with roof drainage

(Beyhan, Erbas 2013). Green roofs can prevent flash floods by reducing the volume of drainage and keeping drainage below the peak (Shafique, Kim, Kyung-Ho 2018).

The GSF, which was first developed in Germany, later started to be applied in many countries (Reinwald et al. 2019). The Green Spaces Factor constitutes a flexible and innovative planning tool that quantifies and assesses the quality of ecological and climatic functions of private green infrastructure. The purpose of the GSF is to ensure that no developed area is falling short of the minimum standard, and it might therefore be necessary to utilize vertical walls and roofs as green space. It aims at increasing the quality of urban landscaping by setting certain development standards.

Calculation of GSF value via the GEE cloud-computing platform will be a valuable tool for translating landscape design standards to planning regulations. Its ease of use, responsiveness, flexibility, and transferability potential are reasons behind its popularity. The results from the preliminary investigation of GSF's applicability in the Turkey planning framework demonstrate that the GSF can successfully regulate the green infrastructure of both new and existing development in urban areas. Therefore, it can contribute positively to improving the environment of densely-built and vegetation-deprived Turkey cities. Unlike current landscaping regulations, GSF retains its regulatory role while allowing the developer to choose how to meet the minimum standards. This can be particularly useful in the context of Turkey planning, where the existing voluminous legislation, by imposing stiff measures and generic geometric constraints, is often unresponsive to the context of each specific development case.

In this study, a green roof proposal was made in order to reduce the negative effects of the flood disaster in the city of Ankara. Since the existing buildings in the study area are generally private property areas and residential areas, green roof applications can only be done through a comprehensive program, and the state, local governments and different stakeholders need to come together and work with a holistic approach.

References

ATİK, A., ASLAN, F., YILMAZ, B., ATEŞ, O. (2013): Modelling purchasing demand of urban people for ornamental plants using logistic regression analysis: sample of Malatya City. Journal of Animal and Veterinary Advances, 12, 16, 1317–1324.

BARNES, K.B., MORGAN, J., ROBERGE, M. (2001): Impervious surfaces and the quality of natural and built environments. In Baltimore, MD: The Department of Geography and Environmental Planning, Towson University.

BARR, C.M., GALLAGHER, P.M., WADZUK, B.M., WELKER, A.L. (2017): Water Quality Impacts of Green Roofs Compared with Other Vegetated Sites. Journal of Sustainable Water in the Built Environment, 3, 3, 4017007.

BECKER, W.R., LÓ, T.B., JOHANN, J.A., MERCANTE, E. (2021): Statistical features for land use and land cover classification in Google Earth Engine. Remote Sensing Applications: Society and Environment, 21, 100459.

BENGTSSON, L., GRAHN, L., OLSSON, J. (2005): Hydrological function of a thin extensive green roof in southern Sweden. Hydrology Research, 36, 3, 259–268.

BERNDTSSON, J.C. (2010): Green roof performance towards management of runoff water quantity and quality: A review. Ecological Engineering, 36, 4, 351–360.

BEYHAN, F., ERBAS, M. (2013): A Study on Green Roofs with the Examples from the World and Turkey. Gazi University Journal of Science, 26, 2, 303–318.

BRUDERMANN, T., SANGKAKOOL, T. (2017): Green roofs in temperate climate cities in Europe–An analysis of key decision factors. Urban Forestry & Urban Greening, 21, 224–234.

CARTER, T.L., RASMUSSEN, T.C. (2006): Hydrologic behavior of vegetated roofs 1. JAWRA Journal of the American Water Resources Association, 42, 5, 1261–1274.

CHANG, C.-C. (2011): LIBSVM: a library for support vector machines, ACM Transactions on Intelligent Systems and Technology, 2, 27, 1--27.

CONNELLY, M., LIU, K. (2005): Green roof research in British Columbia: An overview. Proc. of 3rd North American Green Roof Conference: Greening Rooftops for Sustainable Communities, Washington, DC, 4–6.

DUNNETT, N., KINGSBURY, N. (2008): Planting Green Roofs and Living Walls. Portland, London: Timber Press Inc.

DÜZENLİ, T. (2018): Kentsel Dönüşüme Natif Bir Yöntem: Yeşil Çati Tasarimi. International Journal of Social Humanities Sciences Research (JSHSR), 5, 20, 745–752.

ESRINGÜ, A., TOY, S. (2021). Kent İklimine Çatı ve Cephe Bahçelerinin Etkisi. Climate and Health Journal, 1, 2, 101–107.

FARR, T.G., ROSEN, P.A., CARO, E., CRIPPEN, R., DUREN, R., HENSLEY, S., KOBRICK, M., PALLER, M., RODRIGUEZ, E., ROTH, L. (2007): The shuttle radar topography mission. Reviews of Geophysics, 45, 2.

FASSMAN-BECK, E., VOYDE, E., SIMCOCK, R., HONG, Y.S. (2013): 4 Living roofs in 3 locations: Does configuration affect runoff mitigation? Journal of Hydrology, 490, 11–20.

FIORETTI, R., PALLA, A., LANZA, L.G., PRINCIPI, P. (2010): Green roof energy and water related performance in the Mediterranean climate. Building and Environment, 45, 8, 1890–1904.

FOODY, G.M., MATHUR, A. (2004): Toward intelligent training of supervised image classifications: directing training data acquisition for SVM classification. Remote Sensing of Environment, 93, 1–2, 107–117.

FRAMPTON, W.J., DASH, J., WATMOUGH, G., MILTON, E.J. (2013): Evaluating the capabilities of Sentinel-2 for quantitative estimation of biophysical variables in vegetation. ISPRS Journal of Photogrammetry and Remote Sensing, 82, 83–92.

GEE (2021): Earth Engine Data Catalog. Google Earth Engine. https://developers.google.com/earth-engine/datasets (16.09.2021).

GORELICK, N., HANCHER, M., DIXON, M., ILYUSHCHENKO, S., THAU, D., MOORE, R. (2017): Google Earth Engine: Planetary-scale geospatial analysis for everyone. Remote Sensing of Environment, 202, 18–27.

GRANT, G. (2017): Greater London Authority Urban Greening Factor for London. https://www.london.gov.uk/sites/default/files/urban_greening_factor_for_london_final_report.pdf (16.09.2021).

HU, T., YANG, J., LI, X., GONG, P. (2016): Mapping urban land use by using landsat images and open social data. Remote Sensing, 8, 2, 151.

IENCO, D., INTERDONATO, R., GAETANO, R., MINH, D.H.T. (2019): Combining Sentinel-1 and Sentinel-2 Satellite Image Time Series for land cover mapping via a multi-source deep learning architecture. ISPRS Journal of Photogrammetry and Remote Sensing, 158, 11–22.

JAFARI, N., UTABERTA, N., YUNOS, M.Y.M., ISMAIL, N.A., ISMAIL, S., ARIFFIN, N.F.M., JAFARI, N., VALIKHANI, M. (2015): Benefits of roof garden in order to usage of urban agriculture at roof garden in high-rise building in Malaysia. Advances in Environmental Biology, 9, 24, 86–92.

JANSSON, M. (2014): Green space in compact cities: the benefits and values of urban ecosystem services in planning. NA, 26, 2.

JENSEN, J.R., LULLA, K. (1987): Introductory digital image processing: A remote sensing perspective. Geocarto International, 2, 1, 65.

JULIE, K., KRAGH, K. (2017): GIS and the Green Space Factor. Using GIS to create a baseline for the Green Space Factor in Copenhagen Municipality: Using GIS to create a baseline for the Green Space Factor in Copenhagen Municipality. Aalborg University.

KAYMAZ, I. (2019): The Lost Streams of Ankara: A Case Study of Bentderesi. IOP Conference Series: Materials Science and Engineering, 603, 5, 52040.

KOÇ, G., NATHO, S., THIEKEN, A.H. (2021): Estimating direct economic impacts of severe flood events in Turkey (2015–2020). International Journal of Disaster Risk Reduction, 58, 102222.

KÖHLER, M., SCHMIDT, M., GRIMME, F.W., LAAR, M., DE ASSUNÇÃO PAIVA, V.L., TAVARES, S. (2002): Green roofs in temperate climates and in the hot-humid tropics – far beyond the aesthetics. Environmental Management and Health.

LEE, J.Y., MOON, H.J., KIM, T.I., KIM, H.W., HAN, M.Y. (2013): Quantitative analysis on the urban flood mitigation effect by the extensive green roof system. Environmental Pollution, 181, 257–261.

LI, W.C., YEUNG, K.K.A. (2014): A comprehensive study of green roof performance from environmental perspective. International Journal of Sustainable Built Environment, 3, 1, 127–134.

LI, W., DONG, R., FU, H., WANG, J., YU, L., GONG, P. (2020): Integrating Google Earth imagery with Landsat data to improve 30-m resolution land cover mapping. Remote Sensing of Environment, 237, 111563.

MANTERO, P., MOSER, G., SERPICO, S.B. (2005): Partially supervised classification of remote sensing images through SVM-based probability density estimation. IEEE Transactions on Geoscience and Remote Sensing, 43, 3, 559–570.

MOUNTRAKIS, G., IM, J., OGOLE, C. (2011): Support vector machines in remote sensing: A review. ISPRS Journal of Photogrammetry and Remote Sensing, 66, 3, 247–259.

PAL, M., MATHER, P.M. (2005): Support vector machines for classification in remote sensing. International Journal of Remote Sensing, 26, 5, 1007–1011.

PARK, S., IM, J., PARK, S., YOO, C., HAN, H., RHEE, J. (2018): Classification and mapping of paddy rice by combining Landsat and SAR time series data. Remote Sensing, 10, 3, 447.

Planet Team (2018): Planet Application Program Interface: Space for Life on Earth, https://api.planet.com (16.09.2021).

POURSANIDIS, D., CHRYSOULAKIS, N., MITRAKA, Z. (2015): Landsat 8 vs. Landsat 5: A comparison based on urban and peri-urban land cover mapping. International Journal of Applied Earth Observation and Geoinformation, 35, 259–269.

PRATICÒ, S., SOLANO, F., DI FAZIO, S., MODICA, G. (2021): Machine Learning Classification of Mediterranean Forest Habitats in Google Earth Engine Based on Seasonal Sentinel-2 Time-Series and Input Image Composition Optimisation. Remote Sensing, 13, 4, 586.

QU, L., CHEN, Z., LI, M., ZHI, J., WANG, H. (2021): Accuracy improvements to pixel-based and object-based lulc classification with auxiliary datasets from Google Earth engine. Remote Sensing, 13, 3, 453.

REINWALD, F., RING, Z., KRAUS, F., KAINZ, A., TÖTZER, T., DAMYANOVIC, D. (2019): Green Resilient City – A framework to integrate the Green and Open Space Factor and climate simulations into everyday planning to support a green and climate-sensitive landscape and urban development. IOP Conference Series: Earth and Environmental Science, 323, 1, 12082.

SADEH, Y., ZHU, X., DUNKERLEY, D., WALKER, J.P., ZHANG, Y., ROZENSTEIN, O., MANIVASAGAM, V.S., CHENU, K. (2021): Fusion of Sentinel-2 and PlanetScope time-series data into daily 3 m surface reflectance and wheat LAI monitoring. International Journal of Applied Earth Observation and Geoinformation, 96, 102260.

Sentinel-1 (n.d.). European Space Agency. Retrieved September 14, 2020, from https://sentinel.esa.int/web/sentinel/missions/sentinel-1 (16.09.2021).

SHAFIQUE, M., KIM, R., KYUNG-HO, K. (2018): Green roof for stormwater management in a highly urbanized area: the case of Seoul, Korea. Sustainability, 10, 3, 584.

SHUSTER, W.D., BONTA, J., THURSTON, H., WARNEMUENDE, E., SMITH, D.R. (2005): Impacts of impervious surface on watershed hydrology: A review. Urban Water Journal, 2, 4, 263–275.

SOZER, B., KOCAMAN, S., NEFESLİOGLU, H.A., FİRAT, O., GOKCEOGLU, C. (2018): Preliminary investigations on flood susceptibility mapping in Ankara (Turkey) using modified analytical hierarchy process (M-AHP).

SWAN, A. (2010): How increased urbanisation has induced flooding problems in the UK: A lesson for African cities? Physics and Chemistry of the Earth, Parts A/B/C, 35, 13–14, 643–647.

TAVUS, B., KOCAMAN, S., GOKCEOGLU, C., NEFESLİOGLU, H.A. (2018): Considerations on the use of Sentinel-1 data ın flood mapping in urban areas: Ankara (Turkey) 2018 floods. International Archives of the Photogrammetry, Remote Sensing & Spatial Information Sciences.

Turkish State Meteorological Service (2022): Extreme Maximum, Minimum and Average Temperatures Measured in Long Period, https://www.mgm.gov.tr/eng/forecast-cities.aspx (16.09.2021).

VAN WOERT, N.D., ROWE, D.B., ANDRESEN, J.A., RUGH, C.L., FERNANDEZ, R.T., XIAO, L. (2005): Green roof stormwater retention: effects of roof surface, slope, and media depth. Journal of Environmental Quality, 34, 3, 1036–1044.

VARTHOLOMAIOS, A., KALOGIROU, N., ATHANASSIOU, E., PAPADOPOULOU, M. (2013): The green space factor as a tool for regulating the urban microclimate in vegetation-deprived Greek cities. International Conference on "Changing Cities": Spatial, Morphological, Formal & Socio-Economic Dimensions, Skiathos Island.

VILLARREAL, E.L., BENGTSSON, L. (2005): Response of a Sedum green-roof to individual rain events. Ecological Engineering, 25, 1, 1–7.

WANG, L., DIAO, C., XIAN, G., YIN, D., LU, Y., ZOU, S., ERICKSON, T.A. (2020): A summary of the special issue on remote sensing of land change science with Google earth engine.

WANG, Y., LI, Z., ZENG, C., XIA, G.-S., SHEN, H. (2020): An urban water extraction method combining deep learning and Google Earth engine. IEEE Journal of Selected Topics in Applied Earth Observations and Remote Sensing, 13, 768–781.

WENG, Q., QUATTROCHI, D.A. (2006): Urban Remote Sensing. CRC Press. Elsevier.

YANAR, T., KOCAMAN, S., GOKCEOGLU, C. (2020): Use of Mamdani fuzzy algorithm for multi-hazard susceptibility assessment in a developing urban settlement (Mamak, Ankara, Turkey). ISPRS International Journal of Geo-Information, 9, 2, 114.

ORCID

SİMA POUYA
https://orcid.org/0000-0001-6419-1756

MAJID AGHLMAND
https://orcid.org/0000-0003-0534-5393

FEVZİ KARSLI
https://orcid.org/0000-0002-0411-3315